



Supplementary Information for

Long-range regulation of p53 DNA binding by its intrinsically disordered N-terminal activation domain

Alexander S. Krois, H. Jane Dyson and Peter E. Wright

Peter E. Wright

Email: wright@scripps.edu

This PDF file includes:

Figs. S1 to S7

Table S1

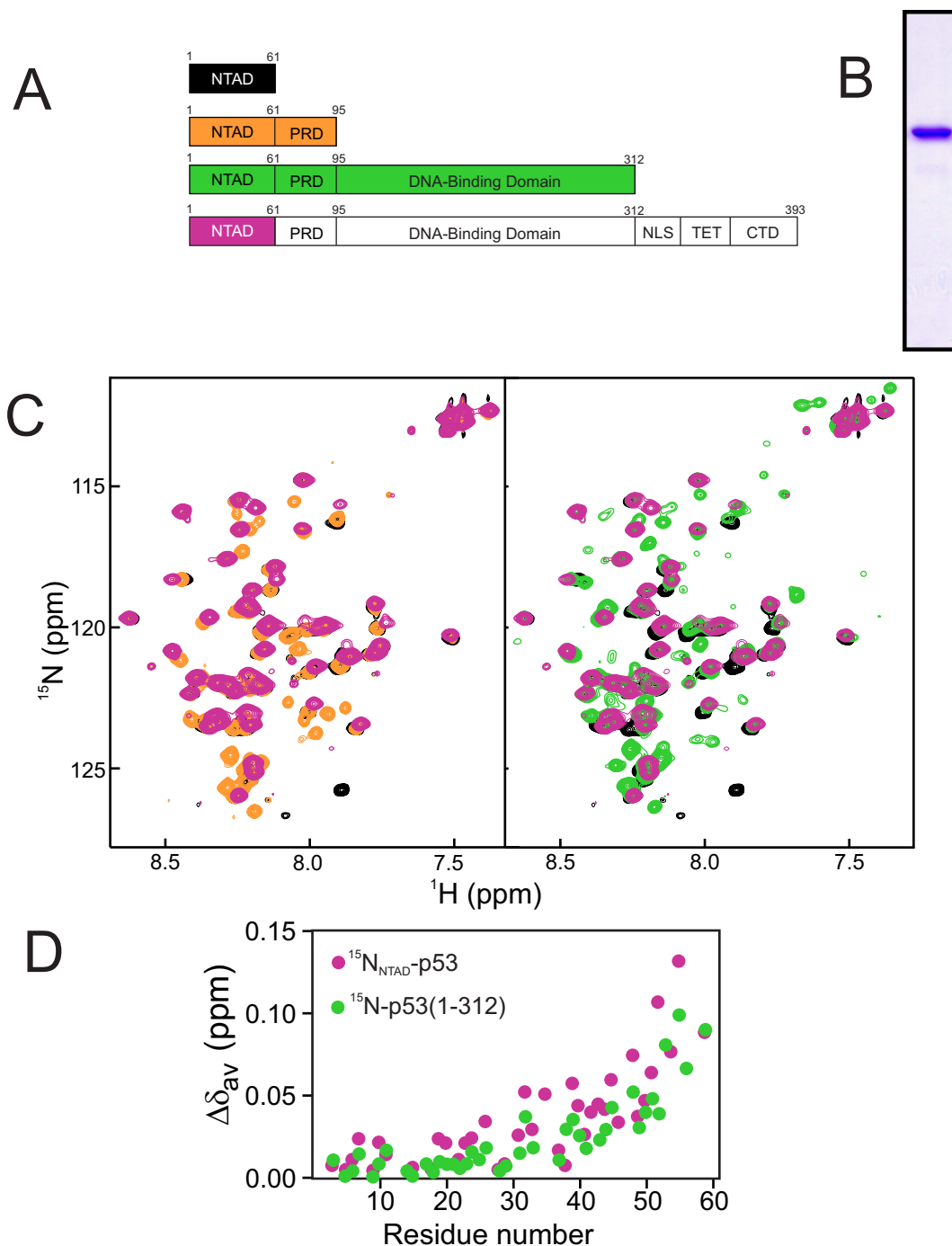


Figure S1. A. Schematic diagram showing the labeled proteins and domains represented in the spectra of part C. B. Coomassie-stained SDS-PAGE gel showing purity (~95% by densitometry) of $^{15}\text{N}_{\text{NTAD}}$ -p53. C. ^1H - ^{15}N HSQC spectra of isolated NTAD (1-61, black) and segmentally-labeled full-length p53 ($^{15}\text{N}_{\text{NTAD}}$ -p53) (purple). The left panel shows an overlay of the ^{15}N NTAD-PRD (1-95, orange). The right panel shows an overlay of the ^{15}N NTAD-PRD-DBD (1-312, green). D. Weighted average NTAD ^1H and ^{15}N chemical shift differences between isolated ^{15}N -NTAD peptide and $^{15}\text{N}_{\text{NTAD}}$ -p53 (purple circles) and between the isolated peptide and ^{15}N NTAD-PRD-DBD (1-312, green circles). Sample conditions as in Figure 1.

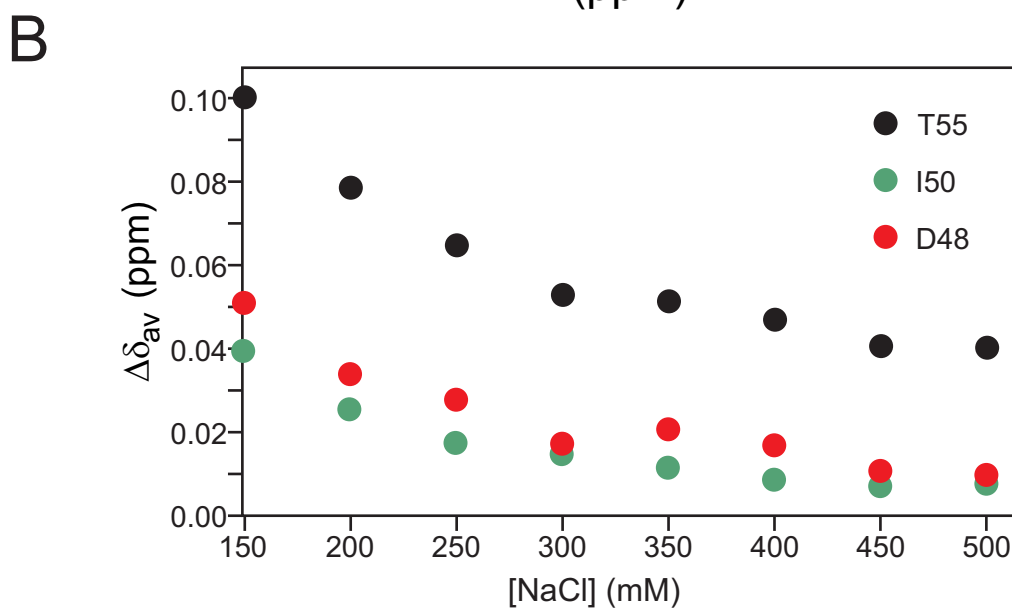
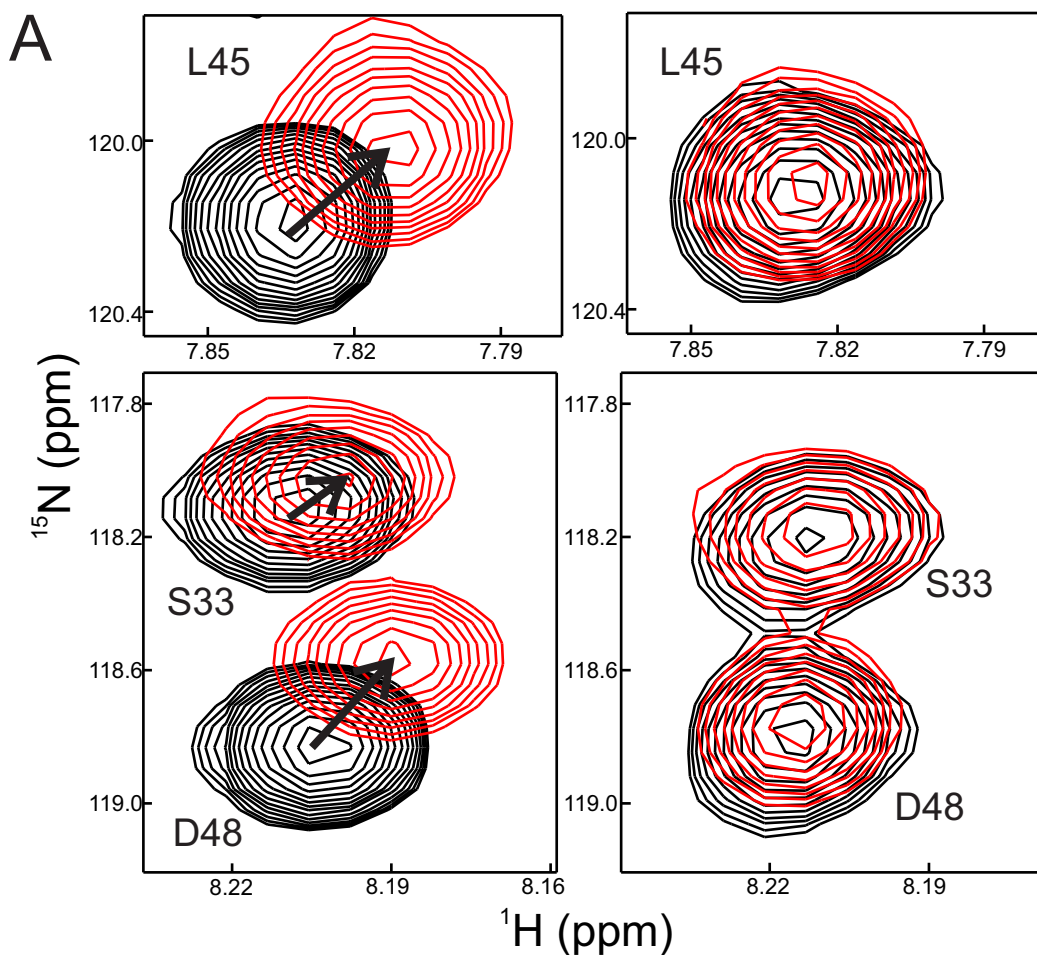


Figure S2. High salt concentrations disrupt the NTAD:DBD interaction. A. Selected regions of 700 MHz ^1H - ^{15}N HSQC spectra of isolated p53 NTAD (residues 1-61) (black) and of p53 (1-312) (red) with 150mM NaCl (left panels) and with 500 mM NaCl (right panels). B. Weighted average chemical shift difference between NTAD(1-61) and p53(1-312) as a function of increasing NaCl concentration for selected residues. Samples were in 20mM Tris, pH 7.0, 2mM DTT, 5% D_2O , with NaCl concentrations shown.

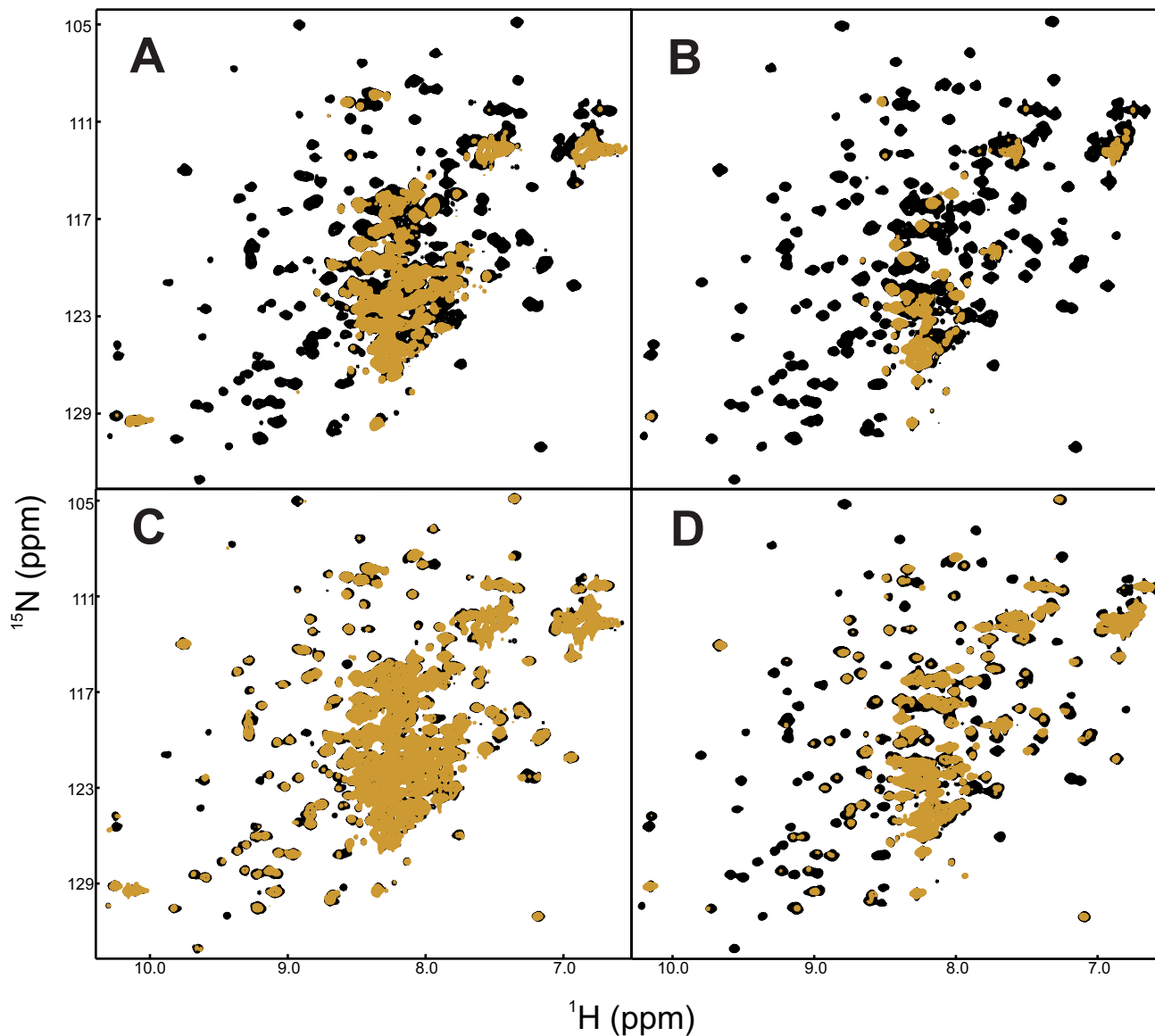


Figure S3. The specificity of DNA binding to the p53 monomer is affected by the NTAD. A. ^1H - ^{15}N HSQC spectra of ^{15}N -labeled p53(1-312) in the absence (black) and presence (gold) of a 0.25x equivalent of a 20 base pair cognate DNA containing specific binding sites for four p53 DBDs. B. ^1H - ^{15}N HSQC spectra of ^{15}N -labeled p53(62-312) in the absence (black) and presence (gold) of a 0.25x equivalent of a 20 base pair cognate DNA containing specific binding sites for four p53 DBDs. For both constructs, the dispersed cross peaks arising from residues in the DBD are broadened beyond detection upon formation of the complex with specific DNA. C. ^1H - ^{15}N HSQC spectra of ^{15}N -labeled p53(1-312) in the absence (black) and presence (gold) of 0.25x equivalents of a 20 base pair non-specific DNA. D. ^1H - ^{15}N HSQC spectra of ^{15}N -labeled p53(62-312) in the absence (black) and presence (gold) of 0.25x equivalents of a 20 base pair non-specific DNA. The dispersed DBD resonances are broadened in the absence (D) but not in the presence of the NTAD. The intense, overlapped cross peaks in the center of the spectra are from NTAD and PRD residues. Sample conditions as in Figure 1.

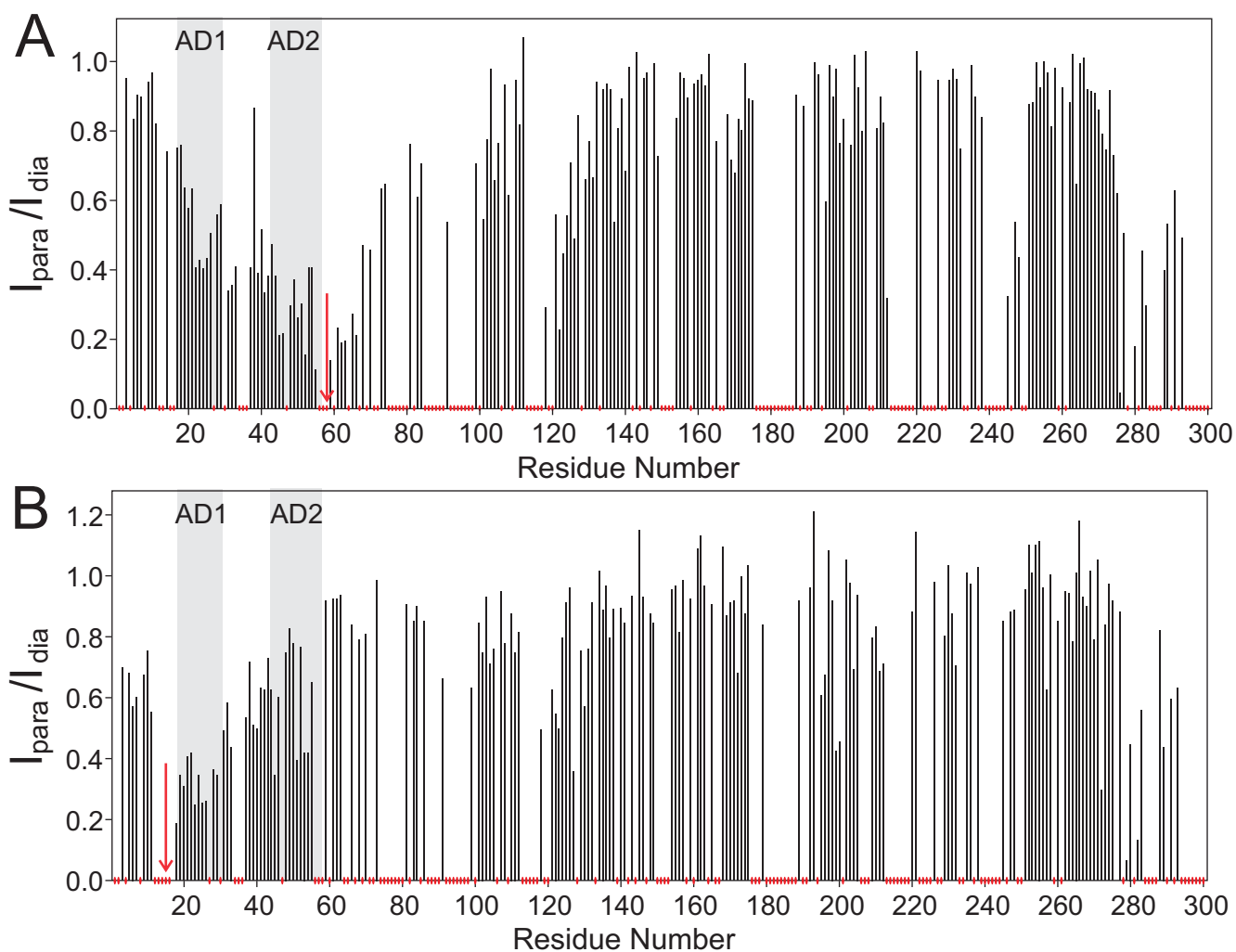


Figure S4. Histograms showing the ratio of the intensity of cross peaks in the ^1H - ^{15}N HSQC spectra of spin-labeled p53(1-312) between the protein containing active (paramagnetic) spin label, and the same protein where the spin label had been deactivated by the addition of ascorbic acid, a reducing agent. A. Spin label at P58C. B. Spin label at S15C. Attachment site is shown by a vertical red arrow. Red ticks on the x-axis denote proline residues and those that were overlapped.

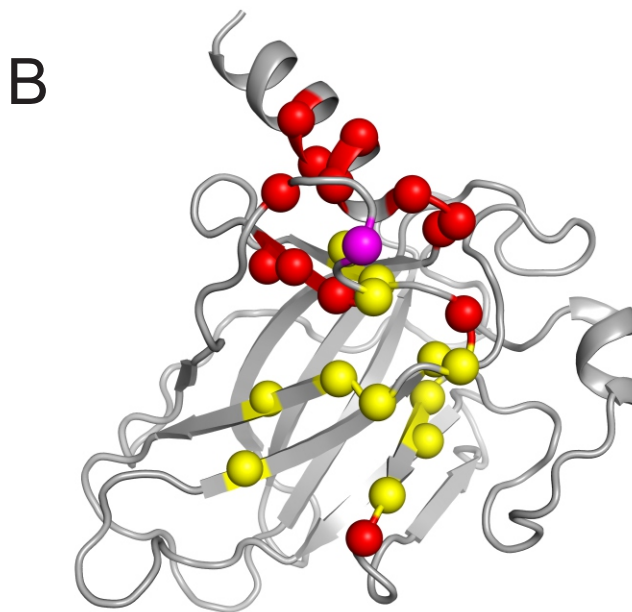
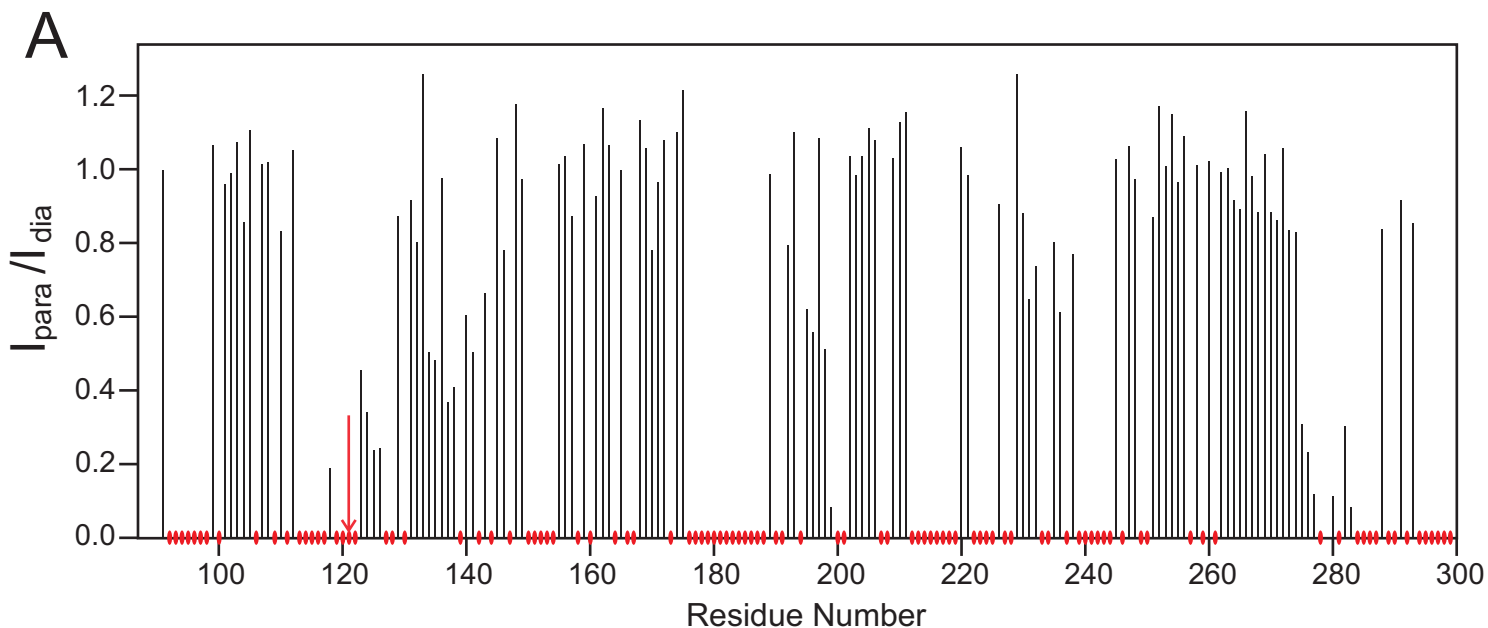


Figure S5. A. Histogram showing the ratio of the intensity ratio of cross peaks in the ^1H - ^{15}N HSQC spectra of residues 90-300 of p53(1-312) spin-labeled at S121C. [Results for residues 1-91 are shown in Figure 7B]. Attachment site is shown by a vertical red arrow. Red ticks on the x-axis denote proline residues and those that were overlapped. B. PRE results for spin-labeled S121C mapped onto the structure of the p53 DBD (PDB: 2XWR). S121, the spin label site, is shown in magenta. Red and yellow spheres correspond to backbone nitrogens for residues that experience greater than 2x the average loss of peak intensity (red) or between 2x and 1x the average loss (yellow) in the presence of the active (paramagnetic) spin label.

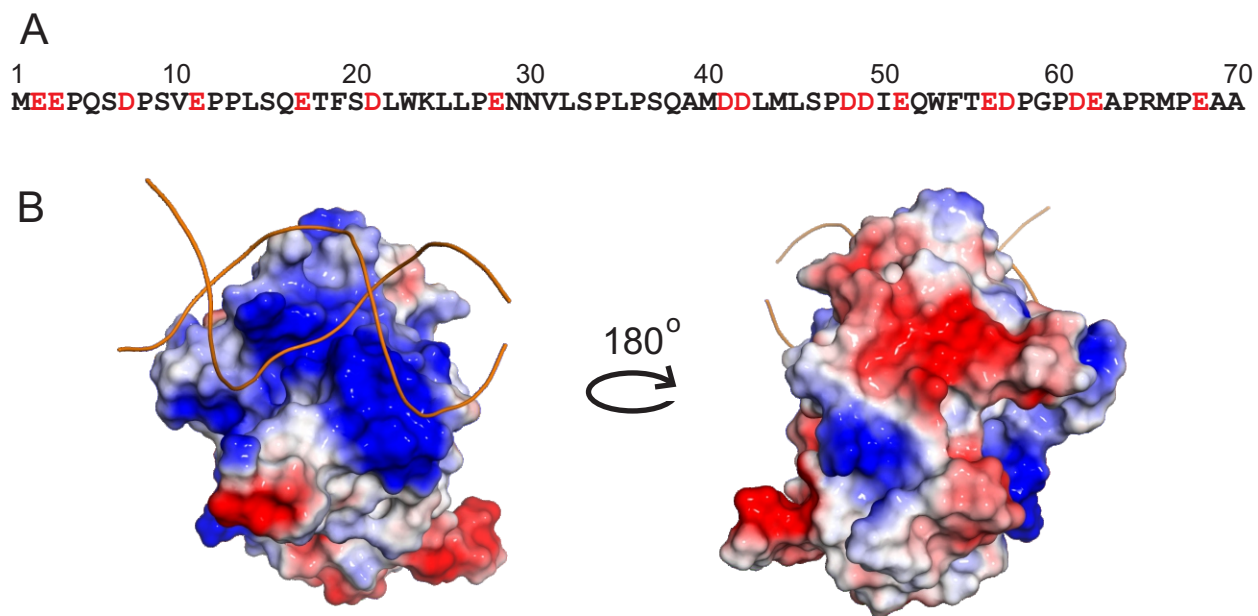


Figure S6. Interactions between the NTAD and DBD involve complementary charges. A. Sequence of the p53 NTAD with acidic residues highlighted in red. B. Electrostatic surface representation of the p53 DBD showing region of positive charge in blue and region of negative charge in red. The phosphate backbone of bound DNA is shown as an orange ribbon. The figure was generated using Pymol (Schrodinger LLC).

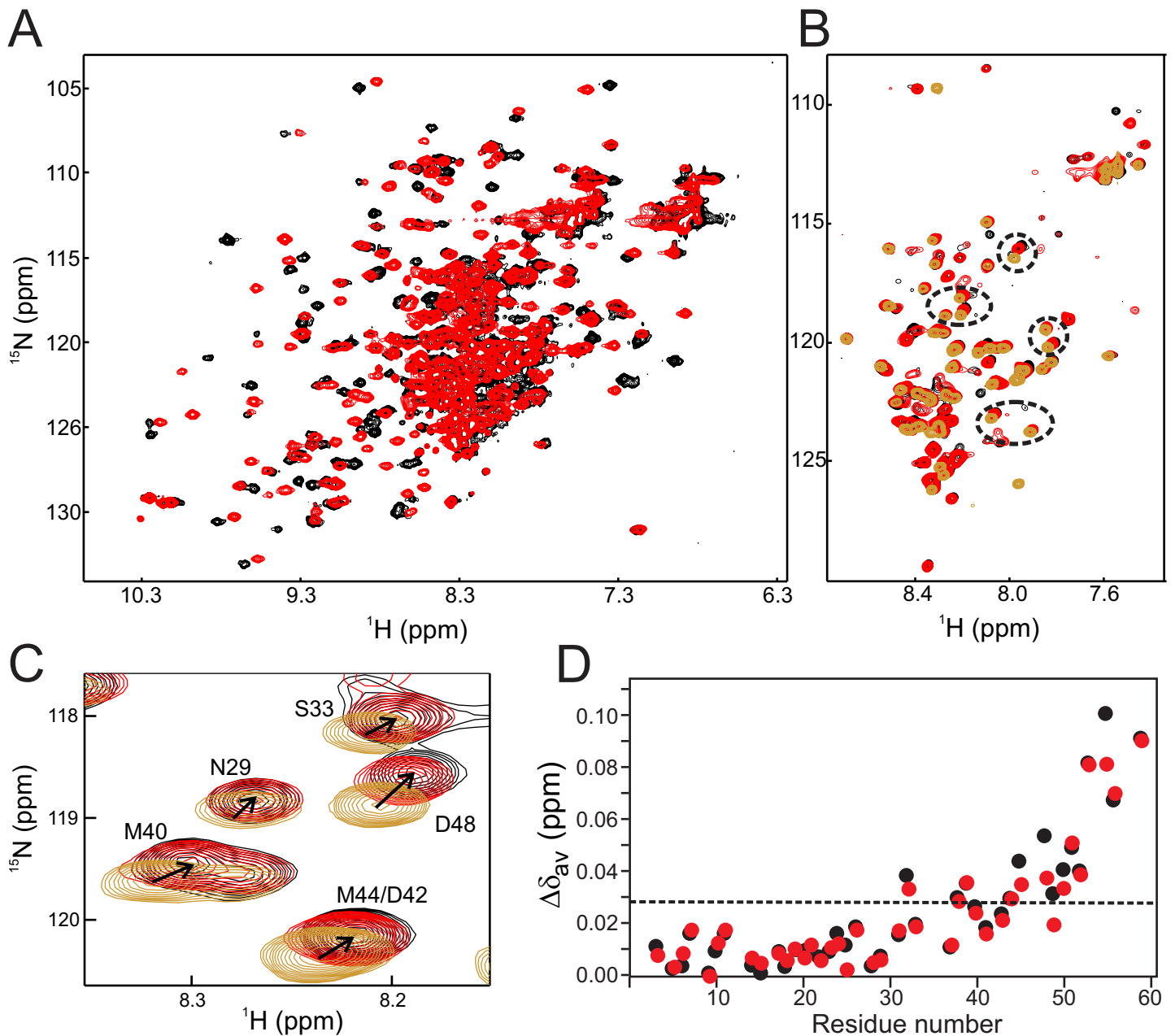


Figure S7. NTAD:DBD interactions are preserved in WT p53. A. ^1H - ^{15}N HSQC spectra of p53(1-312) wild type (black) and 'super-stable' mutant (M113L/V203A/N239Y/N268D) (red) contoured to a low level to visualize DBD resonances. B. The same spectra contoured to a high level to visualize NTAD resonances, overlaid with the spectrum of the isolated NTAD domain (residues 1-61) (gold). C. Expanded region of panel B showing cross peak shifts, with color scheme the same as B. D. Weighted average chemical shift difference between p53(1-312) and isolated p53 NTAD (residues 1-61) for WT (black) and super-stable (red). Dashed line represents the average chemical shift difference between p53(1-61) and p53(1-312) super-stable.

Table S1. Diffusion coefficients and expected molecular weights for p53 constructs.

Protein Construct	Monomer Weight (kDa)	Expected total weight (kDa)	Diffusion coefficient (m ² /s x 10 ⁻⁷)
Uniformly Labeled p53	43.9	175.8	4.3 ± 0.6
NTAD-labeled p53	44.6	178.4	4.1 ± 0.3